A Study of Precision Forging of Steel Spur Gears: Upper Bound Model and Experiments

M. Irani [1], R. Amini Najafabadi[2], T. Dallali Isfahani[3]*
Department of Materials Science and Engineering, Golpayegan University of Technology, Isfahan, Iran

Abstract

Precision forging process is widely used for the production of spur gears due to its advantages such as improved strength and surface finish, little waste of materials and reduction in the machining time of the gear. An important aspect of precision forging process is the load required to perform the process successfully and design the forging tools. In this research, a new kinematically admissible velocity field was presented to predict the precision forging pressure of the steel spur gear by upper bound analysis. The model considered the shape of tooth profile, the number of teeth and friction coefficient. The accuracy of the model was verified using experimental results and a good agreement was found between the two sets of results at the filling stage of the precision forging process. Also, the results were compared with the models developed by other researchers, showing that the teeth profile considered in this study was much closer to the actual profile of the gear.

Keywords: Steel; Precision forging; Upper bound method; Spur Gear.

1. Introduction

Gears are commonly used machine components in power transmission for many applications such as automotive and aerospace [1, 2]. In recent years, there has been a growing interest in the production of gears by the precision forging process to achieve a high production rate and improved strength and surface finish [3, 4]. In the precision forging of spur gears, the complete filling of the die cavity is regarded as the most important factor that can improve the dimensional accuracy and strength of the forged gears. Another important aspect of the gear forging process is the estimation of the load required to perform the process successfully and design the forging tools [5].

Exact solutions are not available for many metal forming processes and several attempts have been made to propose approximate methods which could be adopted for estimating the loads required to cause plastic deformations [6]. In order to estimate the forging load, different methods such as the slab analysis, the upper bound technique [7], and the finite element method [8, 9] have been used by other researchers.

To analyze the precision forging of spur gears, a variety of assumptions have been considered by different researchers to develop the analysis. Grover and Juneja have analyzed [10] the forging of a spur gear shaped component assuming the tooth profile as trapezoidal. Using an upper bound solution, Abdul and Dean 5) investigated the clamping type a forging spur gear in which the tooth profile was parallel to the centerline of the tooth. Chitkara and Kim [11, 12] and Chitkara and Bhutta [13-15] modeled the deformation of different gear-like parts using both the upper bound analysis and the slab method. In order to assess the forging of hollow billets, Jongung Choi et al [16, 17] presented a mathematical method based on the upper bound theory by assuming an involute curve to represent the sides of the gear tooth.

In the present research, a new upper bound analysis was performed using the cylindrical co-ordinate (r, θ, z) to predict the forging pressure of the steel billet within a teethed die cavity for the precision forging process. The profile shape of the tooth was assumed to be tapered from the base circle to the addendum circle. The flow in the tooth region, which was limited between the root and base circles, was only considered to be radial. The predicted forging pressures were compared with those obtained from experiments conducted on commercially prepared lead as the model material for the production of a spur gear of 5 teeth.

2. Theoretical Analysis

The upper bound solution is generated assuming a kinematically admissible velocity field which satisfies the boundary conditions of velocity, continuity and volume constancy [11]. In this work, in order to develop an upper bound solution for the precision forging

**Corresponding author:*
Tel: +98 31 5740065
Email: irani@gut.ac.ir
Address: Department of Materials Science and Engineering, Golpayegan University of Technology
1. M.Sc.
2. Assistant Professor
3. Assistant Professor

of spur gears, deformation was considered to be axi-symmetric. The billet was divided into similar sections of 2N (Fig. 1(a)), where N represents the number of teeth. Each section was then subdivided into 4 different deforming regions, as shown in Fig. 1(b). The following assumptions were made throughout the analysis:

- The material is isotropic, homogeneous and rigid, thereby obeying the von Mises yield criterion.
- The diameter of the billet is equal to that of the root circle of the gear.
- The friction factor between the work piece and die is constant.
- The elastic deformation of the punch and the forging die is neglected.
- The punch moves at a constant speed.

Fig.1(b) shows a deformation unit (OABCDEMN) bounded by two planes of symmetry (OA and OE with α angle between them). No shearing can take place along the planes of symmetry. Hence, deformation within a unit can be assumed as self-contained without any interaction with the adjacent units throughout the forging process. Therefore, the material in the unit displaced by the punch can be considered to form half a tooth.

Radial flow cannot take place in region 1 because of the constraint imposed by the part of the die wall forming the root of the forged tooth (AB in Fig. 1(b)). Thus, the material can tangentially flow from region 1 to 2 as deformation proceeded. The material from region 1 entered region 2 and the material displaced radially by the punch movement in region 2 flows to region 3. Furthermore, in region 3, the material only flows in radial direction and entered region 4, where the profile shape of the gear tooth can be assumed to be tapered (CD in Fig 1(b)).

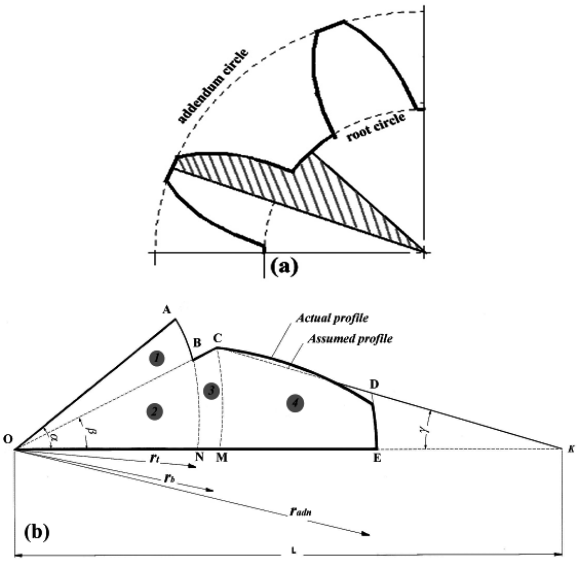

Fig. 1. (a) Schematic representation of a part of a typical spur gear and (b) Deformation zones of a half tooth (shaded area in Fig. 1a) of the gear.

The strain rate field and the volume constancy can be defined using equations (1-a) to (1-e) as shown below:

$$\dot{\varepsilon}_{\theta\theta} = \frac{1}{r}\left(\frac{\partial U_\theta}{\partial \theta} + U_r\right) \tag{1-a}$$

$$\dot{\varepsilon}_{rr} = \left(\frac{\partial U_r}{\partial r}\right) \tag{1-b}$$

$$\dot{\varepsilon}_{zz} = \left(\frac{\partial U_z}{\partial z}\right) \tag{1-c}$$

$$\dot{\varepsilon}_{r\theta} = \frac{1}{2}\left(\frac{1}{r}\frac{\partial U_r}{\partial \theta} + \frac{\partial U_\theta}{\partial r} - \frac{U_\theta}{r}\right) \tag{1-d}$$

$$\dot{\varepsilon}_{rr} + \dot{\varepsilon}_{\theta\theta} + \dot{\varepsilon}_{zz} = 0 \tag{1-e}$$

Regarding the von Misses yield criterion, the plastic, frictional and shear powers can be derived using the following relations[18];

$$\dot{E}_{s,ij} = \int_s \frac{1}{\sqrt{3}}\bar{\sigma}|\Delta V|ds \tag{2-a}$$

$$\dot{E}_{pi} = \int_v \bar{\sigma}\bar{\varepsilon}dv \tag{2-b}$$

$$\dot{E}_{f,i} = \int_{Af} \frac{m}{\sqrt{3}}\bar{\sigma}|\Delta V|dA \tag{2-c}$$

2.1. Zone 1

Radial flow can not take place in zone 1 because of the constraint imposed by the part of the die wall forming the root of the forged tooth (AB in Fig. 1(b)). Therefore, the radial velocity field should be considered as zero:

$$U_r = 0 \tag{3}$$

The circumferential velocity field U_θ could be derived using volume constancy in cylindrical coordinates as shown below:

$$\frac{\partial U_r}{\partial r} + \frac{U_r}{r} + \frac{1}{r}\frac{\partial U_\theta}{\partial \theta} + \frac{\partial U_z}{\partial z} = 0 \Rightarrow$$
$$\frac{1}{r}\frac{\partial U_\theta}{\partial \theta} = \frac{u}{t} \Rightarrow U_\theta = \left(\frac{u}{t}\right)r\theta + C$$

C constant can be calculated by applying boundary conditions. Therefore, U_θ is given by Eq. (4)

$$\theta = \alpha, U_\theta = 0 \Rightarrow U_\theta = -u\left[\frac{(\alpha - \theta)}{t}\right]r \tag{4}$$

2.2. Zone 2

Zone 2 is surrounded by the OCM (see Fig. 1(b)). Circumferential velocity along OC discontinuity surface is the same as that in zone 1

$$U_\theta = -u\left[\frac{(\alpha - \beta)}{t}\right]r \tag{5}$$

Circumferential velocity in zone 2 varies from a maximum amount along OC to zero along OM. Therefore, it can be defined as a linear function of according to Eq. (6):

$$U_\theta = -u\left[\frac{(\alpha-\beta)}{t\beta}\right]r\theta \tag{6}$$

By using circumferential velocity and volume constancy, the radial velocity in this zone can be expressed as Eq. (7):

$$rU_r = u\left[\frac{\alpha}{2t\beta}\right]r^2 + C \tag{7}$$

By considering boundary conditions, U_r can be obtained as shown in Eq. (8):

$$r = 0, U_r = 0 \Rightarrow C = 0, U_r = u\left[\frac{\alpha}{2t\beta}\right]r \tag{8}$$

2.3. Zone 3

The material enters zone 2 from zone 1 while the material is subsequently displaced radially by the punch movement in zone 2, thereby causing a flow to zone 3. In this zone, the material can only flow in the radial direction. Therefore:

$$U_\theta = 0 \tag{9}$$

$$U_r = \frac{ur}{2t} + \frac{(1-\beta)}{\beta}\frac{ur_t^2}{2tr} \tag{10}$$

2.3. Zone 4

To achieve suitable velocity field in zone 4, the radial movement of the material in this zone can be assumed to take place towards apex K. The profile shape of the gear tooth is assumed to be tapered (CD in Fig 1(b)). In this zone, the velocity field has both the radial and circumferential components as shown in Eq. (11) and Eq. (12):

$$U_\theta = \frac{r(\gamma-\theta)\theta}{t\gamma} \tag{11}$$

$$U_r = \frac{r\theta}{t\gamma} - \frac{(L-r_b)\cos\gamma}{r\cos\theta}\left[U_m + \frac{\theta(L-r_b)\cos\gamma}{\gamma t\cos\theta}\right] \tag{12}$$

U_m

is the mean velocity at which the material leaves zone 3 at surface CM and enters into zone 4. It is derived by Eq. (13);

$$U_m t r_b \sin\beta = \frac{\pi r_b}{2N^2},\ \ \alpha = \frac{\pi}{N} \ \ \Rightarrow U_m = \frac{\alpha r_b}{2t\sin\beta} \tag{13}$$

By assuming that the punch speed in z direction is the axial velocity field in zone 1 to 4 can be defined as shown in Eq. (14):

$$U_z = -\frac{u}{t}z \tag{14}$$

The strain rate field could be obtained using equations (1-a) to (1-d). Regarding the von Misses yield criterion, the plastic, frictional and shear powers can be derived using equations (2-a) to (2-c).

To determine the forging load, the total power dissipation, which is the sum of different powers (each power is used with its appropriate equation), can be evaluated using a numerical method with the help of a computer.

3. Materials and methods

The validity of the theoretical analysis was verified by a series of experiments carried out on commercially prepared lead billets. Lead has been extensively used as a material for experimental models, since it presents similar physical properties and shows nearly the same flow pattern as that of steel during deformation at high temperatures [19]. Fig.2 shows the gear die cavity made by W-EDM (wire cut EDM machine) from H13 steel.

Fig.2. The die cavity used to forge spur gears. Fig.2. The die cavity used to forge spur gears.

The forging punch or the top die was of the same size with the same number of teeth as the female die. The specifications of the produced spur gear are presented in Table 1.

Table 1. Specifications of the spur gear dies.

No. of teeth	5
Module	2.25
Pressure angle	20°
Modification coefficient	0.0
Standard pitch circle diameter	12.1
Base circle diameter	11.36

The precision forging test was performed using a press machine with the ram speed of 5 mm/min. The gears were made using billets having almost the exact volume of the material required for the final size of the gear. The billet had a diameter of 8mm, equal to the root diameter of the gear, and a height of 33 mm.

A sample of the billets and the precision forged gear are shown in Fig. 3.

Fig 3. The billet and the precision forged gear.

4. Results and Discussion

Tensile test was carried out on the lead billets at room temperature to evaluate their flow stress. The true stress- strain curve of the lead billet is depicted in Fig.4.

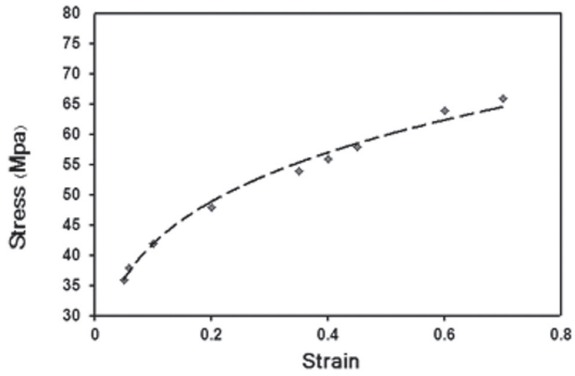

Fig 4. Stress- strain curve of the commercially prepared lead alloy at room temperature.

The $\overline{\sigma}$ parameter, used in the upper bound solution, was taken as the mean flow stress of the billet material and determined using the following true stress- strain relation:

$$\overline{\sigma} = 71.5\overline{\varepsilon}^{0.2} MPa \qquad (15)$$

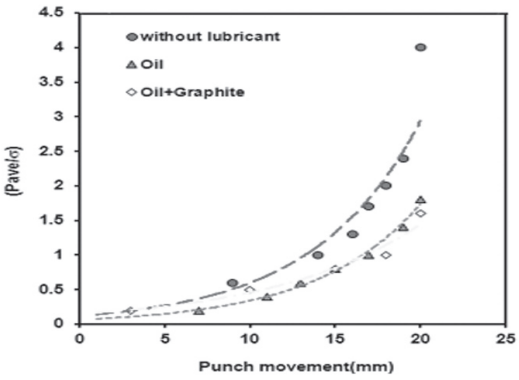

Fig.5. The relative forging pressure of the billets at different lubrication conditions.

Fig. 5 shows the experimental results of the relative forging pressure versus the punch movement for the lead billets at different lubrication conditions. As can be observed, friction at the tool-material interface was affected noticeably by the forging pressure at the final stage of forging, where the teeth of the gear were formed.

Fig. 6 compares the predicted forging pressure of the billet with the experimental results assuming constant friction factors of m=0.1 to m=0.4. It can be seen that predicted results were in a good agreement with the experimental ones at the final stage of the forging process. Moreover, as the lubrication condition was changed, the agreement was achieved at a different m value. In other words, the oil and graphite lubricant provided a friction factor of 0.1 while the "without lubrication condition", matched a friction factor of 0.4.

As can be seen, the rate of increasing the forging pressure was enhanced after the height reduction of about 60%. In other words, two different stages in the forging pressure could be identified; an initial stage where the evolution of the forging pressure was smooth, similar to that that generally occurring in the heading operation, and a final stage where the forging pressure was increased sharply. The latter stage could be attributed to the filling of the teeth [12].

As can be observed, at the beginning of the forging, the predicted forging pressures were higher than their corresponding experimental ones. However, at the filling stage of the forging, the predicted pressures were in a reasonable agreement with the experimental results at a friction factor of m=0.2. The difference between the experimental and predicted pressures at the initial stage of forging could be attributed to the nature of velocity fields defined according to the final shape of the gear [5]. Obviously, the model could not reasonably predict the forging pressure at the initial stages of forging.

Fig.7(a) compares the relative forging pressure predicted by this model with the models developed by Abdul et al [5] and Chitkara & Bhutta [13]. The experimental forging pressure of billets, as reported by Chitkara & Bhutta, is also shown in this figure. To make the results comparable, all models were solved for forging a spur gear of 4 teeth at m=0.2. The tooth profiles considered in these models are shown schematically in Fig. 7(b).

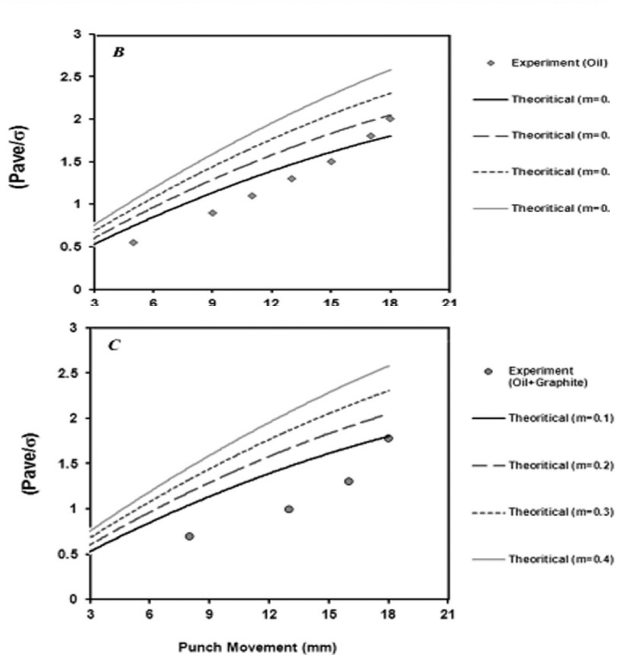

Fig. 6. Comparison of the predicted and experimental relative forging pressures of the billet: (A) without using lubricant, (B) using oil as lubricant and (C) using oil and graphite powder as the lubricant.

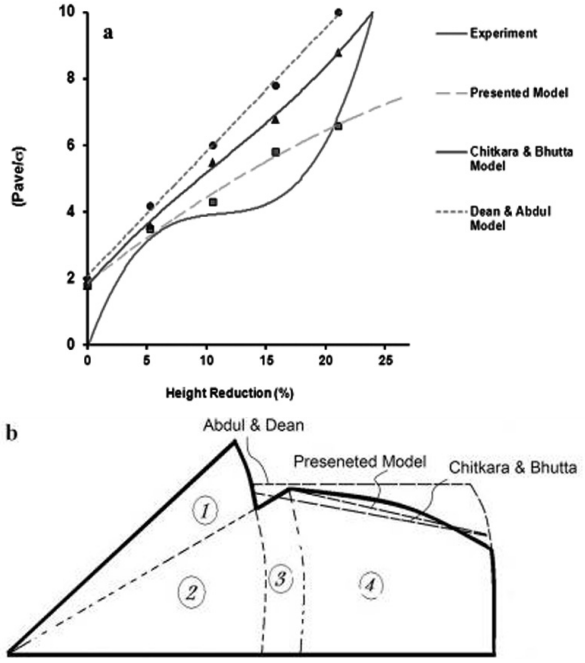

Fig. 7. Comparison of the presented model with other upper bound models: (a) the variation of the predicted relative forging pressure using m=0.2 and (b) the schematic representation of the tooth profiles considered by different models.

In the model presented in this research, we considered a tooth profile much closer to the actual profile of the gear as compared to other models. To do so, an extra velocity region was defined in the model as shown by region 3. It can be seen in Fig. 1b that this region was between the root and the base circles of the gear where the metal flow was only considered to be radial. It can be seen from Fig. 7(a) that the model presented in this paper had a closer prediction of the forging pressure as compared to other models. This result was expected since the assumed tooth profile was much more similar to the actual tooth profile of the gear. It should be noted that at the final stage of forging, the pressure rose very steeply due to the flash formation. None of the models had simulated this stage. So a height reduction less than 20% should be considered to access the accuracy of the models in the prediction of the forging pressure.

5. Conclusion

A new kinematically admissible velocity field for the precision forging of spur gears was proposed to predict the forging pressure by the upper bound technique. The predicted results were compared with the experimental ones achieved to produce a five teeth spur gear. The tests were performed on commercially prepared lead billets at room temperature. A good agreement was found between the two sets of results at the final stage of forging.

ACKNOWLEDGEMENT

The authors would like to thank the Research Board of Golpayegan University of Technology for the financial support and provision of the research facilities used in this work.

References

[1] P. Yogesh , P. Anand: Eng. Failure Analys., 34(2013), 69.
[2] B. X Wang: J. Iron Steel Res. Int., 14(2007), 69.
[3] J.C. Choi, Y. Choi: Int. J Mach. Tool and Manu., 38(1998),1193.
[4] J.C. Choi, Y. Choi: Int. J. Mach. Tool and Manu., 9(1999), 1575.
[5] N. A. Abdul, T. A. Dean: Int. J. Mach. Tool Des. Res., 26(1986), 113.
[6] T. ALtan: Computer simulation to predict load, stress and metal flow in an aximetric closed- die forging in metal forming. Plenner Press,(1971).
[7] H. Haghighat, G.R. Asgari: Int. J. of Mech. Sci., 53(2011), 248.
[8] B. Avitzur: The application of limit Analysis. Marcel Dekker. Metal Forming: New York, (1980).
[9] H. Kudo: Int. J. Mech. Sci., 2(1960), 102.
[10] O. P. Grover, B. L. Junega: Adv. Tech. Plasticity., 11(1984).
[11] N.R. Chitkara, Y. Kim: Int. J. Mech. Sci., 38(1996), 777.
[12] N.R. Chitkara, Y. Kim: Int. J. Mech. Sci., 38(1996), 791.

[13] N. R. Chitkara, M.A. Bhutta: Int. J. Mech. Sci., 38(1996), 916.
[14] N.R. Chitkara, M. A. Bhutta: Int. J. Mech. Sci., 37(1995), 1247.
[15] N.R. Chitkara, M. A. Bhutta: Int. J. Mech. Sci., 38(1996), 871.
[16] J. Choi, H. Cho, C.Y. Jo: J. Mater. Process. Technol., 104(2000), 104, 67.
[17] J. Choi, H. Cho, C.Y. Jo: J. Mater. Process. Technol., 104(2000), 104, 1.
[18] R. L. Bodnar, D.C. Ronemus: Physical modeling of hot deformation processes using plasticine, Trams, 1996, 35.

Abbreviations

$\dot{E}_{p,i}$: internal energy dissipation rate in the ith zone

$\dot{E}_{s,i,j}$: energy dissipation rate along velocity discontinuity surface between the ith and jth zones

$\dot{E}_{f,i}$: energy dissipation rate due to friction at the tool-metal interface in the ith zone

$\dot{E}_t$: total energy dissipation rate

N : number of teeth

P : die pressure

r_t, r_b, r_{add}: radius of the root, base and addendum circle

t :height of the work piece

U_r, U_θ, U_z : radial, circumferential and axial velocity components

U_m : mean velocity

u : punch velocity

α, β, γ : angles, see Fig 1

$\dot{\bar{\varepsilon}}_i$: effective strain rate in the ith zone

$\dot{\varepsilon}_{rr}, \dot{\varepsilon}_{\theta\theta}, \dot{\varepsilon}_{zz}$:radial, circumferential and axial strain rate components

$\dot{\varepsilon}_{r\theta}$: shear strain rate

ΔV :velocity discontinuity

$\bar{\sigma}$: flow stress

m : friction factor